

Verification of an Improved Computational Design Procedure for TWT-Dynamic Refocuser-MDC Systems with Secondary Electron Emission Losses

PETER RAMINS, HENRY G. KOSMAHL, FELLOW, IEEE, DALE A. FORCE, MEMBER, IEEE, RAYMOND W. PALMER, AND JAMES A. DAYTON, JR., SENIOR MEMBER, IEEE

Abstract—A computational procedure for the design of TWT-refocuser-MDC systems was used to design a short “dynamic” refocusing system and highly efficient four-stage depressed collector for a 200-W 8–18-GHz TWT. The computations were carried out with advanced multidimensional computer programs which model the electron beam as a series of disks of charge and follow their trajectories from the RF input of the TWT, through the slow-wave structure and refocusing section, to their points of impact in the depressed collector. Secondary emission losses in the MDC were treated semiquantitatively by injecting a representative beam of secondary electrons into the MDC analysis at the point of impact of each primary beam. A comparison of computed and measured TWT and MDC performance showed very good agreement. The electrodes of the MDC were fabricated from a particular form of isotropic graphite that was selected for its low secondary electron yield, thermal expansion characteristics, ease of machinability, and vacuum properties. This MDC was tested at CW for more than 1000 h with negligible degradation in TWT and MDC performances.

NOMENCLATURE

B_z	Axial magnetic field in teslas.
I_b	Intercepted beam current in amperes.
I_G	Total body current, including backstreaming from collector in amperes.
I_0	Beam current in amperes.
P_{RF}	Total RF output power in watts.
V_0	Cathode potential with respect to ground in volts.
η_c	TWT circuit efficiency, $P_{RF}/(P_{RF} + \text{circuit losses})$.
η_{col}	Collector efficiency.
η_{ov}	Overall TWT efficiency, $P_{RF}/(\text{dc input power})$.
η_{RF}	TWT RF efficiency, $P_{RF}/(V_0 I_0)$.

I. INTRODUCTION

IN EARLIER PAPERS [1], [2] published in this journal, a computational procedure for the design of TWT-refocuser-MDC systems was presented. The present paper extends this work to short permanent magnet “dynamic” refocusing systems (simultaneous beam debunching and re-

conditioning) using the TWT computer program, to a semiquantitative treatment of secondary electron emission losses, and to collectors of very small size. Furthermore, the performance of a new collector electrode material, a particular form of isotropic graphite (POCO Graphite, Inc., DFP-2), is described.

The work was conducted at the NASA Lewis Research Center under a joint NASA-USAF program to improve the performance of TWT's for use in communications and electronic countermeasure systems. The improved computer-aided design technique was used to design a short permanent magnet refocuser and a very small (1.7-cm diam.) four-stage depressed collector for an existing Varian 200-W 8–18-GHz TWT (VA Model VTM-6294). The refocusing system and MDC designs were implemented, and an experimental program was conducted to evaluate the TWT/MDC performance. In the following, the analytical and experimental procedures and the tube characteristics are briefly described; the results of the TWT, refocusing system, and MDC analyses are discussed; and, comparisons of analytical and experimental results are presented. The performance of the isotropic graphite electrode material is briefly described.

II. TWT CHARACTERISTICS

A modified version of Varian TWT model VTM-6294 was used in this program. This tube has a helical slow-wave circuit and PPM focusing. The general tube operating characteristics were as follows:

frequency:	8–18 GHz
beam voltage:	9.2–9.8 kV
beam current:	0.23–0.26 A
RF output power:	200 W minimum
duty cycle:	100 percent (CW).

III. ANALYTICAL AND EXPERIMENTAL PROCEDURE

The computational design procedure was used to design a refocusing system and a four-stage depressed collector for the VA TWT, with small size, simplicity, and ease of fabrication in mind. The TWT computer analysis was done at saturation at the midband frequency of 13 GHz (where

Manuscript received May 10, 1985; revised July 24, 1985.
P. Ramins, D. A. Force, R. W. Palmer, and J. A. Dayton are with the NASA Lewis Research Center, Cleveland, OH 44135.
H. G. Kosmahl was with the NASA Lewis Research Center, Cleveland, OH 44135. He is now with the Analox Corp., Cleveland, OH 44135.
IEEE Log Number 8405801.

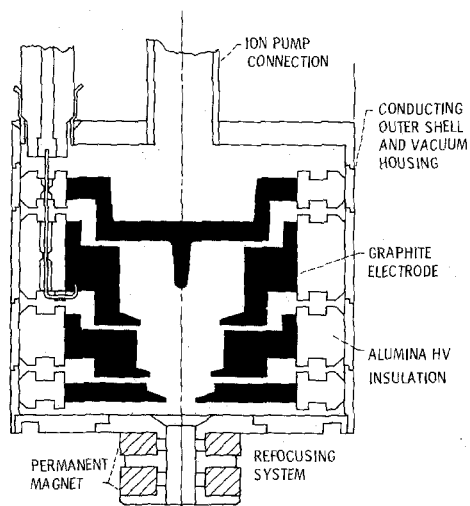


Fig. 1. Cross section of four-stage brazed graphite depressed collector and permanent magnet refocuser.

the greatest electronic efficiency was expected to occur) using the 32-disk model and a recently implemented improved formulation in the modeling of the PPM stack, based on a formulation similar to that in [3].

Since the TWT already had two full-strength permanent magnets beyond the RF output coupler of the TWT, it was decided to attempt to design a refocusing system by making use of this continuation of the PPM stack for 1.25 magnetic periods. Optimization of this simple refocuser by varying the strength of the magnets remained a possibility if satisfactory collector efficiencies were not predicted, but it was not necessary to implement this option. A recent modification in the method of utilization of the TWT program permits the stable computation of the electron-beam flow in a region where the tunnel diameter changes discontinuously. This permits the dynamic analysis of a wide variety of refocusing systems. The effects on the spent beam of debunching and reconditioning in the refocuser can now be computed simultaneously. This more elaborate analysis indicated that this very simple refocuser would work very well, and so it was employed.

The collector was designed, using the Herrmannsfeldt Electron Trajectory Program [4], before the semiquantitative technique for evaluating secondary electron emission losses in collectors was implemented; had this been available, the collector design would have been modified slightly.

This TWT, equipped with the four-stage brazed graphite collector shown in Fig. 1, was fabricated and experimentally evaluated at a number of distinct TWT/MDC operating conditions, including:

- 1) analytical design case collector voltages, and
- 2) experimentally optimized collector voltages.

A comparison of the analytical and measured results for these two operating conditions is presented below. However, because the TWT was not operated first with an undepressed collector (which produces only negligible backstreaming power) and the TWT and the MDC electrodes

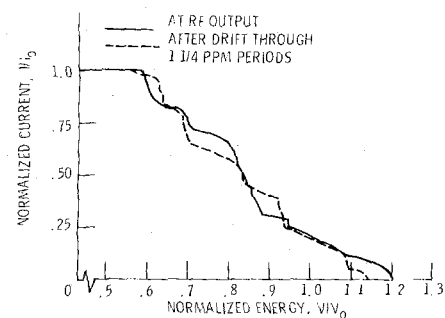


Fig. 2. Computed spent-beam energy distributions before and after debunching for TWT operation at saturation. Electronic efficiency, $\eta_e = 0.16$; perveance is $0.28 \times 10^{-6} \text{ A/V}^{3/2}$.

TABLE I
ANALYTICAL VERSUS EXPERIMENTAL TWT PARAMETERS AND CW PERFORMANCE OF TWT DESIGN CASE AND TWT 204

I. Operating parameters		
Parameter	Design case	TWT 204
Cathode voltage	9.30 kV	9.60 kV
Cathode current	255 mA	240 mA

II. TWT performance at 13 GHz (midband)		
Parameter	Design case	TWT 204
RF efficiency, %	13.5	12.3
Electronic efficiency, %	16.2	16.4
Circuit efficiency, %	83.6	^a 75
Intercepted current, %	4.2	1.9

^aEstimated value based on measurements of other TWT types.

were conduction cooled to a single baseplate, it was not possible to present the detailed picture of power flow in the experimental TWT/MDC given in [1], [2]. Furthermore, the computation of collector efficiencies required the making of certain assumptions (discussed later).

IV. RESULTS OF TWT ANALYSIS AND COMPARISON WITH MEASUREMENTS

The computed and measured RF performances are shown in Table I. Since the tube operating parameters for the analytical design case and the experimental TWT (called TWT 204 hereafter) differed somewhat, the results in this and in subsequent sections of this paper are shown as percentages of I_0 , V_0 , and $I_0 V_0$. The results are in relatively good agreement. The highest RF efficiency, of 13.5 percent, of TWT 204 occurred at 15.0 GHz.

The computed spent-beam energy distributions before and after debunching, for operation of the TWT at saturation, are shown in Fig. 2. As observed previously in [1], [2], the debunching action substantially alters the spent beam energy distribution.

V. REFOCUSING ANALYSIS RESULTS

The beam debunching in the refocuser has already been discussed. The charge trajectories through the refocusing region are shown in Fig. 3. The disk edge angles and average radius at the input to and the output of the refocuser are shown in Table II. The number of negative angles has

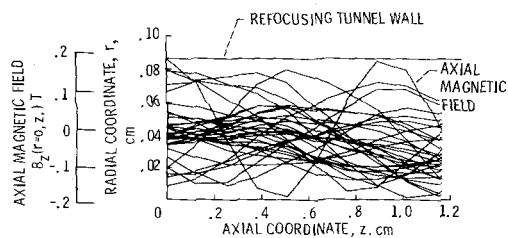


Fig. 3. Charge trajectories and refocusing field profile in refocusing section for TWT operation at saturation.

TABLE II
INPUT AND OUTPUT CHARACTERISTICS OF REFOCUSING SYSTEM FOR SATURATED OPERATION

I. Angle of disk edge.		
Trajectory	Input angle, deg	Output angle, deg
1	-4.3	-1.1
2	1.5	-1.3
3	.1	3.9
4	.8	.2
5	5.2	-.5
6	2.8	.4
7	2.1	-1.8
8	2.7	-4.0
9	1.7	.2
10	1.6	-1.0
11	-2.2	3.9
12	7.1	-7.4
13	2.4	-3.2
14	2.3	.6
15	-.4	1.7
16	1.7	4.4
17	1.4	-1.5
18	.3	-2.0
19	-2.4	1.4
20	-5.1	-3.3
21	-1.2	7.7
22	-.2	3.1
23	-1.2	2.8
24	5.0	-2.3
25	-.5	-3.3
26	-2.3	2.0
27	1.2	7.5
28	3.1	-4.5
29	4.1	-.4
30	2.5	1.6
31	1.0	3.3
32	-.8	-.4

II. Average radius of disk edge.		
	At input, mm	At output, mm
Average radius	0.35	0.28

been increased and the average beam radius reduced (compression rather than the controlled beam expansion described in [1], [2]); on the surface this does not appear to be a good refocusing system. However, as will be shown in the next section, it was possible to design a highly efficient collector for this beam. When the beam size at the MDC input is much smaller than the collector size, positive and negative angles become indistinguishable to the collector; and, for MDC's of such small size, beam expansion may not be desirable. Consequently, this refocusing system was selected for its simplicity and ease of fabrication.

VI. MDC ANALYSIS AND RESULTS AND COMPARISON WITH MEASUREMENTS

The four-stage axisymmetric MDC geometry, the applied potentials, the equipotential lines, and the charge trajectories are shown in Figs. 4 and 5 for the cases of

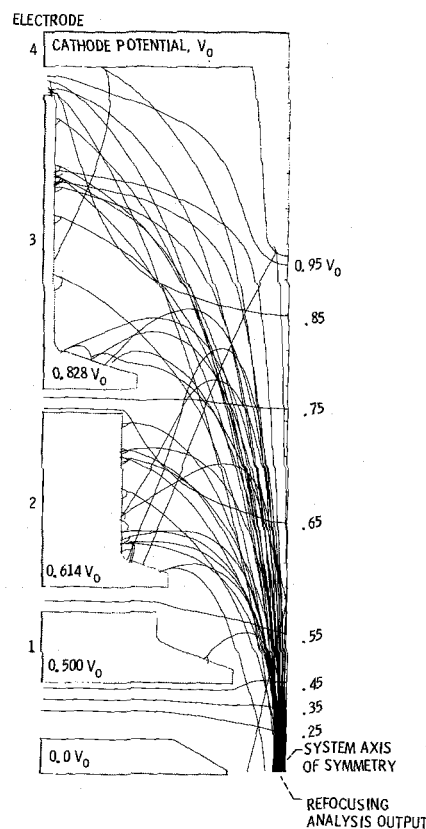


Fig. 4. Charge trajectories in four-stage 1.7-cm-diameter depressed collector operated at analytically determined voltages. TWT operating at saturation.

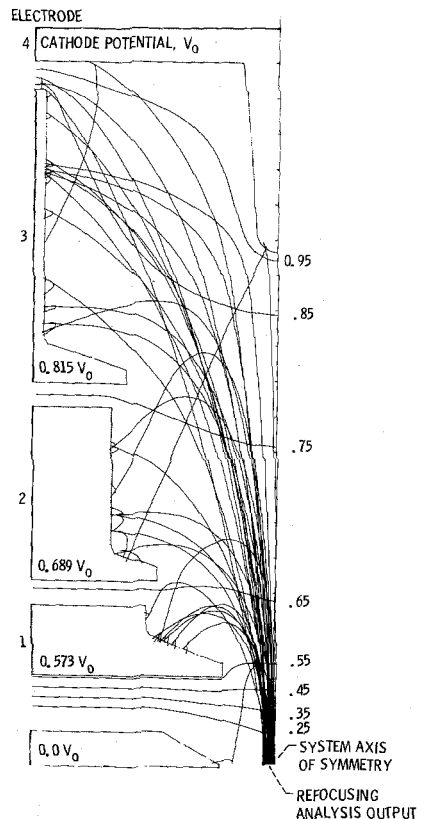


Fig. 5. Charge trajectories in four-stage 1.7-cm-diameter depressed collector operated at experimentally optimized voltages. TWT operating at saturation.

TABLE III

ANALYTICAL AND EXPERIMENTAL PERFORMANCES OF TWT 204 AND 1.7-CM-DIAMETER FOUR-STAGE DEPRESSED COLLECTOR AND TWT OPERATING AT SATURATION (ANALYTICALLY DETERMINED COLLECTOR VOLTAGES) (Computer trajectories shown in Fig. 4. Voltages, currents, and powers in percent of V_0 , I_0 , and $V_0 I_0$, respectively).

Collecting element	Voltage with respect to ground	Analytical		Experimental	
		Current	Recovered power	Current	Recovered power
TWT body (interception)	0	4.1	0	1.9	0
TWT body (backstreaming)	0	4.2	0	1.8	0
Electrode:					
1	50.0	3.1	1.6	5.1	2.6
2	61.4	43.0	26.4	60.0	36.8
3	82.8	42.6	35.2	29.5	24.4
4	100.0	3.0	3.0	1.7	1.7
Collector efficiency, %		82.9		80.2	
Overall efficiency, %		39.9		35.7	

TABLE IV

ANALYTICAL AND EXPERIMENTAL PERFORMANCES OF TWT 204 AND 1.7-CM-DIAMETER FOUR-STAGE DEPRESSED COLLECTOR AND TWT OPERATING AT SATURATION (EXPERIMENTALLY OPTIMIZED COLLECTOR VOLTAGES) (Computed trajectories shown in Fig. 5. Voltages, currents, and powers in percent of V_0 , I_0 , and $V_0 I_0$, respectively).

Collecting element	Voltage with respect to ground	Analytical		Experimental	
		Current	Recovered power	Current	Recovered power
TWT body (interception)	0	4.1	0	1.9	0
TWT body (backstreaming)	0	3.1	0	1.1	0
Electrode:					
1	57.3	21.0	12.7	9.5	5.4
2	68.9	23.2	16.0	53.7	37.0
3	81.5	45.5	37.1	32.2	26.3
4	100.0	3.0	3.0	1.6	1.6
Collector efficiency, %		85.4		86.2	
Overall efficiency, %		42.3		41.6	

analytically determined voltages and experimentally optimized voltages, respectively. The analytical and experimental TWT-MDC performances are compared in Tables III and IV.

The computed collector current distributions shown in Tables III and IV include the effects of representative secondary electron emission from the electrode surfaces. These are for the case of slow (10 eV) electrons injected back along the angle of incidence (the most probable angle in some cases) in the amount $I_i(0.4 + 0.2\theta^2)$, where θ is the angle of incidence in radians and I_i is the incident current. Secondary electrons have, in fact, angular and energy distributions, which depend on the angle of incidence, the energy of the incident electrons, and the electrode surface material and characteristics. A better simulation (other energies and angles of injection) is possible; however, detailed measurements of secondary electron emission characteristics (the angular and energy distributions) of modern MDC electrode materials (e.g., POCO DFP-2 graphite) are generally not available. Furthermore, more complex simulations involve additional computer time and may not be cost-effective.

The trajectories of this one class of slow secondary electrons are shown in Figs. 4 and 5. Most of the secondaries

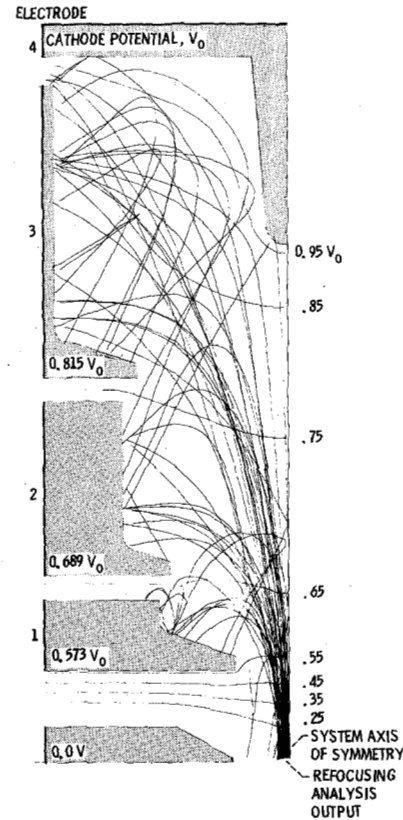


Fig. 6. Charge trajectories of incident and of elastically reflected primaries in four-stage depressed collector. TWT operating at saturation.

are suppressed automatically by the local electric fields. However, Fig. 4 shows that, in some cases (see electrodes 2 and 3), slow secondaries generated even on the "top" surfaces of the electrodes can backstream to the TWT itself. Clearly, such situations should be avoided by modified collector design or electrode operating potentials.

The losses due to elastically and inelastically scattered primary (high energy) electrons may be at least as important as those due to true secondaries; however, only very limited quantitative data have been found on this component of secondary electron emission for electrode materials used in modern collectors.

The trajectories of elastically reflected primary electrons injected at an angle of reflection equal to the angle of incidence are shown in Fig. 6. When other possible angles of injection are considered, it is clear they could end up almost anywhere in the collector or TWT. No attempt was made to quantify these losses due to the lack of data on reflected primaries from POCO DFP-2 graphite.

As discussed previously, since the TWT was not first operated with an undepressed collector, certain assumptions had to be made in order to compute collector efficiencies. The following assumptions were used:

- 1) circuit efficiency of 0.75 at 13 GHz (based on measurements of other TWT types);
- 2) $I_b = 4\frac{1}{2}$ mA (based on measurements for several TWT's of this model with zero collector depression,¹ at very low duty cycle); and

- 3) average energy of intercepted electrons of $0.98 V_0$ (the computed value).

Comparing the predicted and measured currents to the various collector electrodes, it can be seen that the agreement is good only in some of the cases. The differences in computed and measured currents can largely be explained by subtle differences of only 5 to 10 percent in the computed and actual spent beam energy distributions. For example, the computed and measured values of current to electrode number three showed very good agreement (43 versus 44 percent) when the applied voltage to the electrode in the analytical case was decreased by 7 percent.

The collector efficiencies showed very good agreement. This is of particular importance, since the primary purpose of the computer-aided design techniques, apart from TWT performance analysis and design, is to produce an acceptable refocusing-system design and a highly efficient MDC geometric design. Predicting the distribution of current to the electrodes at one particular operating point is of considerably less importance, since the collector and the power supplies must be designed to tolerate a wide range of currents to allow for operation at other conditions, in particular below saturation.

The combination of computer-aided MDC geometric design and experimental optimization of its operating voltages produced a very good design on the first design iteration. At the outset of this program, it was envisioned that the refocusing system profile (strength of the two permanent magnets) would be optimized by individually trimming the strength of the two refocusing system magnets, within the range of ± 10 percent, and by shunting the magnets to optimize the TWT overall efficiency. However, the "packaged" TWT/MDC delivered by Varian did not provide ready access to the refocusing system. Consequently, because of the favorable results obtained with the nominal refocuser, and because of the risk involved in the removal (and subsequent reinstallation) of the coaxial-to-waveguide adapter (a delicate procedure), such optimization was not performed.

VII. TWT-MDC PERFORMANCE ACROSS OPERATING BANDWIDTH

The TWT and four-stage collector performance was evaluated across its useful operating band at saturation. This turned out to be 8–15.5 GHz, limited in the upper end of the band by a *poor output match* for a range of frequencies above 16 GHz. The MDC voltages used (1.0, 0.77, 0.68, and $0.50 V_0$) had to be reduced considerably from their optimum values at midband (see Table IV) due to a large increase in the total body current (backstreaming from the collector) for operation in the range of frequencies of 8.5–10.5 GHz, where a significant second harmonic content is present in the RF output power. The results are shown in Fig. 7. The collector efficiency was found to be in the range of 81–84.5 percent. The average results (across the operating band of 8–15.5 GHz at saturation) are shown in Table V.

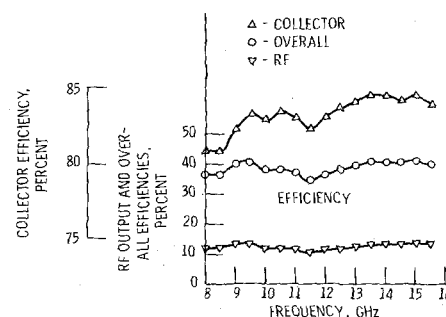


Fig. 7. Collector, overall, and RF efficiencies versus frequency at saturation.

TABLE V
AVERAGE RESULTS OF TWT-MDC PERFORMANCE ACROSS OPERATING BAND OF 8–15.5 GHz AT SATURATION

RF Efficiency (Percent)	Overall Efficiency (Percent)	Collector Efficiency (Percent)
12.5	39	83

In computing the collector efficiencies, the following assumptions were used:

- 1) a linear variation in η_c from 0.8 to 0.725 for frequencies in the range of 8–15.5 GHz, and
- 2) a constant intercepted beam power (1.9 percent of $I_0 V_0$, as discussed above).

VIII. PERFORMANCE OF POCO DFP-2 GRAPHITE AS A COLLECTOR ELECTRODE MATERIAL

The TWT and MDC were assembled, baked out, and dc/RF processed at Varian. The bakeout was performed in two stages (separated by a cathode-activation procedure) for a total of 30 h at 550°C . Approximately 35 h of pulsed dc aging (no RF) and over 30 h of gradual CW RF aging were required before saturated CW data could be obtained across the operating band. A 2-l/s ion pump at the collector (see Fig. 1) was used throughout these tests.

The bakeout performance of the TWT/MDC was indistinguishable from the production TWT with its copper collector; however, the TWT/MDC was described as "gassy" at several early stages in the testing program at Varian. The above information was extracted from the tube log supplied by Varian. In all, more than 100 h of pulsed and CW aging/testing were accumulated at Varian.

During initial testing at NASA Lewis, the 2-l/s ion pump was used continually. Pump currents, which ranged from 0.02 to $0.025 \mu\text{A}$ initially, dropped to virtually zero (less than 5 to 10×10^{-9} A, the minimum detectable on the pump current readout) within about 100 h of operation.

An extended test was started with the TWT operating at saturation at 15 GHz. After about 400 h of CW operation, the ion pump was turned off entirely. In retrospect, this could probably have been done at the start of the long-term test. The testing was continued until over 1000 h of CW operation had been accumulated. A daily check was

made for a possible pressure buildup by turning the pump back on for a few seconds; no measurable pump current was ever detected.

During the first several hundred hours of operation, the total body current was observed to rise (from 3 percent of I_0 to 5 percent) and the recovered power was observed to drop about 20 W, the largest changes occurring early in the extended test program. The RF output power remained constant within 1 percent, but the saturated gain increased slightly. The observed overall efficiency decreased by 1-1.5 percentage points. It could not be definitely established whether the changes in body current and recovered power were due to changes in the TWT itself (larger beam due to improved outgassing of the TWT components), to small dimensional changes in the TWT or MDC, or to changes in the secondary electron emission characteristics of the graphite electrodes.

IX. CONCLUDING REMARKS

An improved computational design technique for TWT-refocuser-MDC systems was presented. A highly efficient MDC design was produced on the first iteration, and very good agreement was found between computed and measured collector efficiencies.

The implementation of the dynamic refocusing analysis makes possible the design of short permanent magnet refocusers situated next to the RF output coupler of the TWT.

The evaluation of secondary electron emission losses in the collector presented above was only semiquantitative. However, the technique itself is capable of much greater accuracy when measurements of the angular and energy distributions from modern MDC electrode materials become available.

Operation of the experimental TWT across its octave bandwidth indicated that the tube produced considerably different spent beams in the midband to upper band parts (highest η_c) and near the low band edge, where a significant amount of harmonic power was generated.

An effective compromise in MDC operating conditions (voltages) was found for saturated TWT operation. However, efficiency in the linear range would have been compromised because the collector voltages had to be reduced. Consequently, it would be useful, in certain cases, to perform the analysis at two or more frequencies, including a frequency near low band edge (with fundamental and harmonic power) and at the highest electronic efficiency.

The new type of graphite MDC electrode material, POCO DFP-2, performed well. However, considerably more experience with it is required before definitive conclusions on its suitability for ECM and space TWT's can be made.

ACKNOWLEDGMENT

The authors wish to express their gratitude to B. Ebihara for the thermal, mechanical, and HV designs of the MDC, and for the MDC fabrication.

REFERENCES

- [1] J. A. Dayton, Jr., H. G. Kosmahl, P. Ramins, and N. Stankiewicz, "Analytical prediction and experimental verification of TWT and depressed collector performance using multidimensional computer programs," *IEEE Trans. Electron Devices*, vol. ED-26, pp. 1589-1598, 1979.
- [2] J. A. Dayton, Jr., H. G. Kosmahl, P. Ramins, and N. Stankiewicz, "Experimental verification of a computational procedure for the design of TWT-refocuser-MDC systems," *IEEE Trans. Electron Devices*, vol. ED-28, pp. 1480-1489, 1981.
- [3] F. Sterzer, and W. W. Siekanowicz, "Design and periodic permanent magnets for focusing of electron beams," *RCA Rev.*, vol. 18, pp. 39-59, 1957.
- [4] W. B. Herrmannsfeldt, "Electron trajectory program," Stanford Linear Accelerator Center, Stanford University, SLAC-166, Sept. 1973.

*

Peter Ramins, photograph and biography not available at the time of publication.

*



Henry G. Kosmahl (SM'59-F'79) attended the Technical University of Dresden and Darmstadt, Germany, from 1940 to 1949, and received the Doctor of Science degree in electron physics for work on high-efficiency klystrons.

Prior to coming to the United States, he was an Instructor of Physics at the University of Darmstadt and also worked at the Electron Tube Laboratory of AEG-Telefunken, Ulm, Germany, on low-noise and transit-time effects in electron streams. From 1967 to 1985 he headed the Power Amplifier Section in the Communications Technology Branch, NASA Lewis Research Center, Cleveland, OH, working on multidimensional electron-beam interaction, depressed collectors, high-efficiency design, unconventional circuits, and space TWT's. He is currently a private consultant on electron-beam devices. He has published over 40 journal articles, has been awarded 12 patents, two pending, two in current use in space and AF-TWT's, and is a consultant to the Air Force and the Cleveland Clinic Foundation.

*

Dale A. Force (M'84) was born in Saginaw, MI, on September 19, 1952. He received the B.S. and M.S. degrees in physics from Michigan State University in 1974 and 1976, respectively.

Since 1983, he has been employed at the NASA Lewis Research Center, Cleveland, OH, where he has been working on multistage depressed collector design.

*

Raymond W. Palmer, photograph and biography not available at the time of publication.

*



James A. Dayton, Jr. (M'59-SM'83) was born in Chicago, IL, on December 22, 1937. He received the B.S. degree in electrical engineering from Illinois Institute of Technology, Chicago, in 1959, the M.S. degree in electrical engineering from the University of Iowa, Iowa City, in 1960, and the Ph.D. degree in electrical engineering from the University of Illinois, Urbana, in 1965.

While at the University of Illinois, he was a Research Assistant in the Gaseous Electronics Laboratory. Upon graduation in 1965, he became a Research Engineer working on plasma diagnostics at Cornell Aeronautical Laboratory. He joined the NASA Lewis Research Center, Cleveland, OH, in 1967, and was assigned to the Microwave Amplifier Section in 1971, where he has been concerned with electron-beam diagnostics, electron-gun design, and multistage depressed collector design. In 1983, he was assigned temporarily to NASA Headquarters, Washington, D.C. as Manager for Communications Technology. He returned to the Lewis Research Center in 1984 to become Head of the Microwave Amplifier Section. He is also a Lecturer in electrical engineering at Cleveland State University.

Dr. Dayton is a member of Phi Eta Sigma, Eta Kappa Nu, Tau Beta Pi, and Sigma Xi. He is a Registered Professional Engineer in the State of Ohio.